DYNAMICS OF AXIALLY MOVING BEAMS MADE OF FUNCTIONALLY GRADED MATERIALS

Marcelo T. Piovan[a] **and Rubens Sampaio**[b]

[a]*Mechanical Systems Analysis Group, Universidad Tecnológica Nacional - Fac. Reg. Bahía Blanca, 11 de Abril 461, Bahía Blanca, BA, 8000, Argentina, e-mail: mpiovan@frbb.utn.edu.ar,*
http://www.frbb.utn.edu.ar

[b]*Department of Mechanical Engineering, Pontifícia Universidade Catôlica - Rio de Janeiro, Rua Marquês de São Vicente 225, Rio de Janeiro, RJ, 22453-900, Brasil, e-mail: rsampaio@mec.puc-rio.br*
http://www.mec.puc-rio.br

Keywords: Axially moving beams, functionally graded materials.

Abstract. Problems related to the vibrations of axially moving flexible beams made of functionally graded materials are addressed. The problem of an axially moving beam may be interpreted as a telescopic system where the mass is not constant, the mechanism of elastic deformation is transverse bending.

A thin-walled beam with annular cross-section is analyzed, where a continuously graded variation in the composition of ceramic and metal phases across the wall thickness with a simple power law is considered.

In this paper a finite element scheme is employed to obtain numerical approximations to the variational equation of the problem. Normally, finite element approaches use fixed-size elements, however for this kind of problems the increase of the number of elements, step by step as the mass enters is a cumbersome task. For this reason an approach based on a beam-element of variable domain is adopted. The length of the element is a prescribed function of the time.

Results highlighting the effects of the beam flexibility, tip mass and material constituents on the dynamics of the axially moving beams are presented and the corresponding conclusions are given.

1   INTRODUCTION

Axially moving beams appear in a broad range of problems such us telescopic robotic manipulators, deployment of flexible antennas or appendages of spacecrafts, band-saw blades as well as the rolling process of plates, wire rods, recorder tapes and belts, among others. In this kind of problems the conservation of mass is not automatically satisfied because it may change depending on the type of boundary conditions. That is, if the axially moving beam is considered to be inextensible or axially rigid and it is supported between two fixed points (the case of belts or band-saw blades), the mass of the system in the domain can be conserved if the motion amplitude is small. However, in the case of telescopic cantilevered beam (the case of robot arms), the mass of the system is not conserved as mass enters or leaves the domain. In this class of problems, the rate of entering mass is a prescribed value. The study of flexible beams in a translational axial movement have been gaining attention in the last years (Stylianou and Tabarrok, 1994; Behdinan et al., 1997a,b; Theodore et al., 1996; Imanishi and Sugano, 2003; Al-Bedoor and Khulief, 1996, 1997), due to new applications in the areas of robotics and spacecrafts (specifically modeling telescopic flexible actuators traveling through prismatic joints). These last applications may operate under severe environmental conditions such as high temperatures, requiring an extended operational life. Under these circumstances, the use of functionally graded materials can offer some constructive answers in order to avoid possible structural limitations.

The functionally graded materials are a kind of composites whose properties vary continuously and smoothly from a ceramic surface to a metallic surface in a specified direction of the structure. The ceramic face protects the metallic surface from corrosion as well as thermal failure, whereas the metallic part offers the strength and stiffness to the structure. The material properties are normally modeled varying according to a power law along the thickness of a shell (Reddy and Chin, 1998) that constitutes the structure. The research in structural problems, focusing attention in the employment of functionally graded materials, has been mainly devoted to eigenvalue analysis of beams (Oh et al., 2003), plates and shells (Reddy and Chin, 1998). However, to the best of author's knowledge, in spite of its importance, no research work related to the vibrations of axially moving flexible beams made of functionally graded materials has been yet presented.

In the present work, a study on the vibrations of flexible sliding beams made of functionally graded materials, deployed or retrieved through a prismatic joint, is performed. The beam is modeled employing Euler-Bernoulli assumptions for small displacements and deformations (Stylianou and Tabarrok, 1994; Theodore et al., 1996). A finite element scheme is employed to obtain numerical approximations to the variational equation of the problem. Normally, finite element approaches use fixed-size elements, however for this kind of problems the increase of the number of elements, step by step as the mass enters is a cumbersome task that needs a very large number of small elements in order to reach reasonable smoothness and accuracy in the results. Other authors (Al-Bedoor and Khulief, 1996, 1997) developed a finite element scheme where a transition element is employed in the link as the mass enters. Although the use of transition element is an interesting idea, however it presents some inconveniences in the programming stage because one has to consider that the element is partially housed in the hub, then without flexural deformation. For this reason an approach based on a beam-element of variable domain developed earlier by other authors (Stylianou and Tabarrok, 1994) is adopted in this work, where the length of the element is a prescribed function of the time. The finite element methodology introduced by those authors is revisited in order to make clear its use in the context

of a beam constructed with functionally graded materials. A study of dynamic responses for different cases of axial deploying patterns and material configurations is performed.

2 STRUCTURAL MODEL

2.1 Basic Assumptions

Figure 1 shows a horizontal flexible beam of variable length $L(t)$ moving along its longitudinal x-axis at a prescribed velocity, $V = \partial_t L(t)$. The beam has a total length L_T, and an annular cross-section, where the material properties are functionally graded in the thickness. The following hypotheses are considered in order to develop the model: (a) Bernoulli-Euler assumptions are invoked to model the structure, i.e. the cross section is preserved from distortions in its plane, rotary inertia effects are neglected and extensional deformation are supposed to be small; (b) the gravitational potential energy due to the elastic deformations is not taken into account in comparison to the overall reference motion; (c) A tip mass is considered to be concentrated at the free end of the beam. (d) The beam is composed by ceramic and metallic phases, where a simple power-law-type definition is employed for the volume fraction of metal (ceramic) in the thickness.
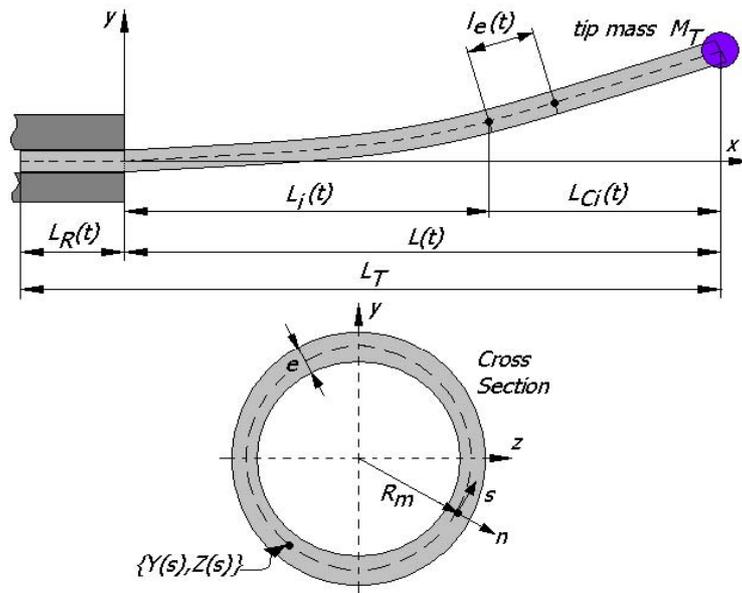

Figure 1: Beam configuration .

The functionally graded shells are considered to be composed by many isotropic homogeneous layers (Tanigawa, 1995). The stress-strain relations for a generally isotropic material including thermal effects are expressed as (Kadoli and Ganesan, 2006):

$$
\left\{
\begin{array}{c}
\sigma_{xx} \\
\sigma_{ss} \\
\sigma_{xn} \\
\sigma_{ns} \\
\sigma_{xs}
\end{array}
\right\}
=
\left[
\begin{array}{ccccc}
Q_{11} & Q_{12} & 0 & 0 & 0 \\
Q_{12} & Q_{11} & 0 & 0 & 0 \\
0 & 0 & Q_{44} & 0 & 0 \\
0 & 0 & 0 & Q_{55} & 0 \\
0 & 0 & 0 & 0 & Q_{66}
\end{array}
\right]
\left(
\left\{
\begin{array}{c}
\varepsilon_{xx} \\
\varepsilon_{ss} \\
\varepsilon_{xn} \\
\varepsilon_{ns} \\
\varepsilon_{xs}
\end{array}
\right\}
-
\left\{
\begin{array}{c}
\hat{\alpha}\Delta T \\
\hat{\alpha}\Delta T \\
0 \\
0 \\
0
\end{array}
\right\}
\right)
\tag{1}
$$

The matrix elements Q_{ij} are defined in terms of effective elastic properties:

$$\begin{aligned}
Q_{11} &= \frac{E_{eff}}{1-\nu_{eff}^2} \\
Q_{12} &= \frac{E_{eff}\nu_{eff}}{1-\nu_{eff}^2} \\
Q_{44} = Q_{55} = Q_{66} &= \frac{E_{eff}}{2\left(1+\nu_{eff}\right)} \\
\hat{\alpha} &= \frac{\alpha_{eff}}{1-\nu_{eff}}
\end{aligned} \tag{2}$$

As the Euler-Bernoulli hypotheses are invoked, only the first two components of stress and strain of equation (1) would be employed.

The effective material properties are given by:

$$E_{eff}(n) = (E_o - E_i)\left(\frac{2n+e}{2e}\right)^K + E_i \tag{3}$$

$$\nu_{eff}(n) = (\nu_o - \nu_i)\left(\frac{2n+e}{2e}\right)^K + \nu_i \tag{4}$$

$$\alpha_{eff}(n) = (\alpha_o - \alpha_i)\left(\frac{2n+e}{2e}\right)^K + \alpha_i \tag{5}$$

$$\rho_{eff}(n) = (\rho_o - \rho_i)\left(\frac{2n+e}{2e}\right)^K + \rho_i \tag{6}$$

$$\kappa_{eff}(n) = (\kappa_o - \kappa_i)\left(\frac{2n+e}{2e}\right)^K + \kappa_i \tag{7}$$

where E_{eff}, ν_{eff}, α_{eff}, ρ_{eff} and κ_{eff} are the effective modulus of elasticity, effective Poisson's coefficient, effective thermal expansion coefficient, effective mass density and effective thermal conductivity coefficient, respectively. These properties are defined for $n \in [-e/2, e/2]$, where e is the thickness. The subindexes "o" and "i" stand for outer and inner surfaces, respectively. $K\,(0 \leq K \leq \infty)$ is the power law exponent. It becomes evident that if $K = 0$ the beam is entirely made of the outer material, normally ceramic. In addition to the exponential laws of variation in the radial direction, the properties may be subjected to variation with the temperature that can be represented in the following expression (Reddy and Chin, 1998):

$$m_p = p_0 \left(p_{-1}T^{-1} + 1 + p_1 T + p_2 T^2 + p_3 T^3\right) \tag{8}$$

where m_p is a material property in general (i.e. modulus of elasticity, or Poisson's coefficient, etc.), T is the absolute temperature and the coefficients p_i are unique for a particular material and obtained by means of a curve fitting procedure (Praveen et al., 1999). Thus the material properties can be represented as a function of the thickness and the temperature.

2.2 Variational Formulation of the Structural Member

The displacement field taking into account the hypotheses of the previous paragraph is:

$$u_x\left(x, s, n, t\right) = -\left[Y(s) - n\frac{dZ}{ds}\right]\frac{\partial v(x,t)}{\partial x}$$

$$u_y\left(x, s, n, t\right) = v\left(x, t\right) \tag{9}$$

The displacement field (9) is a particular case of displacement fields of thin-walled beam formulations (Oh et al., 2003; Cortinez and Piovan, 2002), where the points $\{Y(s), Z(s)\}$ describe the middle line of the wall thickness (see Figure 1). Under the hypotheses proposed in the previous paragraph, only the axial strain is considered, which can be expressed as:

$$\varepsilon_{xx} = \bar{\varepsilon}_{xx} + n\bar{\kappa}_{xx} \tag{10}$$

where $\bar{\varepsilon}_{xx}$ and $\bar{\kappa}_{xx}$ are given by:

$$\bar{\epsilon}_{xx} = -Y(s)\frac{\partial^2 v}{\partial x^2}$$

$$\bar{\kappa}_{xx} = \frac{dZ}{ds}\frac{\partial^2 v}{\partial x^2} \tag{11}$$

Then, the strain energy of this structural member can be described as:

$$E_d = \frac{1}{2}\int_0^{L(t)} J_{11}^{11}\left(\frac{\partial^2 v}{\partial x^2}\right)^2 dx \tag{12}$$

The kinetic energy of the system may be expressed as:

$$E_k = \frac{1}{2}\int_0^{L(t)} J_{11}^{\rho}\left[\left(\frac{\partial v}{\partial t} + \frac{\partial x}{\partial t}\frac{\partial v}{\partial x}\right)^2 + \frac{\partial V}{\partial t}\left(L - x\right)\left(\frac{\partial v}{\partial x}\right)^2\right]dx + \frac{1}{2}J_{11}^{\rho}L_T V^2 \tag{13}$$

In expressions (12) and (13), $L(t)$ is the instantaneous length of the protruded part of the sliding beam. In expression (13), the first term, the underlined term and the double underlined term correspond to the transverse complementary kinetic energy, the kinetic energy due to axial acceleration - also called co-kinetic energy (Behdinan et al., 1997a,b) - and the complementary longitudinal kinetic energy (or kinetic energy due to the axial motion of the rigid body), respectively. This last term is a prescribed quantity since the sliding velocity $V(t)$ is prescribed. It has to be noted that expressions (12) and (13) are similar to the ones of the case of isotropic materials (Stylianou and Tabarrok, 1994). Note also, that in equation (13), $\partial x(t)/\partial t = \partial L(t)/\partial t = V$, due to the condition of inextensibility. The constants J_{11}^{11} and J_{11}^{ρ} are the flexural stiffness and sectional inertia for a functionally graded material, that are given by the following expressions:

$$J_{11}^{11} = \int_0^{2\pi R_m}\left[\bar{A}_{11}Y^2(s) + \bar{D}_{11}\right]ds$$

$$J_{11}^{\rho} = \int_0^{2\pi R_m}\int_{-e/2}^{e/2}\rho_{eff}\,dn\,ds \tag{14}$$

In the above expressions ρ_{eff} is obtained from (6); $\bar{A}_{11}$ and $\bar{D}_{11}$ are modified shell-stiffnesses for functionally graded materials which are obtained eliminating N_{ss} and M_{ss} (which are considered negligible as a common procedure for composites materials (Cortinez and Piovan, 2002; Oh et al., 2003)) and reducing $\bar{\epsilon}_{ss}$ and $\bar{\kappa}_{ss}$ from the following expression:

$$\left\{ \begin{array}{c} N_{xx} \\ N_{ss} \\ M_{xx} \\ M_{ss} \end{array} \right\} = \left[\begin{array}{cccc} A_{11} & A_{12} & B_{11} & B_{12} \\ A_{12} & A_{11} & B_{12} & B_{11} \\ B_{11} & B_{12} & D_{11} & D_{12} \\ B_{12} & B_{11} & D_{12} & D_{11} \end{array} \right] \left\{ \begin{array}{c} \bar{\varepsilon}_{xx} \\ \bar{\varepsilon}_{ss} \\ \bar{\kappa}_{xx} \\ \bar{\kappa}_{ss} \end{array} \right\} \tag{15}$$

where N_{xx} and N_{ss} are shell forces, M_{xx} and M_{ss} are shell moments, and A_{ij}, B_{ij} and D_{ij} are given by:

$$\{A_{ij}, B_{ji}, D_{ij}\} = \int_{-e/2}^{e/2} Q_{ij} \left\{1, n, n^2\right\} dn \tag{16}$$

Since this problem has mass entering (or leaving) the system, normally it is described by means of an Eulerian formulation. However, as it was shown earlier for this kind of problem (Behdinan et al., 1997a; McIver, 1973), the Lagrangian formulation can still be used even for the case of a system with changing mass. In these circumstances, the equation of motion can be obtained by the following Lagrangian expression:

$$\delta\mathcal{L} = \delta E_k - \delta E_d = 0 \tag{17}$$

2.3 Finite Element Discretization

As it was mentioned previously a finite element scheme will be employed to solve the motion equation. The approximation scheme for this sliding beam model for functionally graded materials is based on the concept of variable domain element introduced in the nineties (Stylianou and Tabarrok, 1994) for the case of isotropic materials. In this context, the length of the element is not considered fixed, but varying according to the prescribed sliding velocity V. In order to develop the finite element equation for the variable domain element, the free part of the sliding beam is divided into a number of equal length elements. Under this circumstances, the Lagrangian (17) for a i-th element is given by:

$$\delta\mathcal{L}_i = \frac{\delta}{2} \int_0^{l_e(t)} \left\{ J_{11}^\rho \left[\frac{\partial \bar{v}}{\partial t} + \frac{\partial L_{Ci}}{\partial t} \frac{\partial \bar{v}}{\partial \bar{x}} + \frac{\partial V}{\partial t} \left(L_{Ci} - \bar{x}\right) \left(\frac{\partial \bar{v}}{\partial \bar{x}}\right)^2 \right] - J_{11}^{11} \left(\frac{\partial^2 \bar{v}}{\partial \bar{x}^2}\right)^2 \right\} d\bar{x} = 0 \tag{18}$$

where the overbar in the variables corresponds to the homonym variables but in the element domain. The location of the spatial variable $\bar{x}(t)$ in the element domain, is given by the following expression:

$$\bar{x}(t) = x(t) - L_i(t) \tag{19}$$

Then, since $\partial x(t)/\partial t = \partial L(t)/\partial t = V$, the velocity of position change in the element domain is given by:

$$\frac{\partial \bar{x}(t)}{\partial t} = \frac{\partial x(t)}{\partial t} - \frac{\partial L_i(t)}{\partial t} = \frac{\partial L(t)}{\partial t} - \frac{\partial L_i(t)}{\partial t} = \frac{\partial L_{Ci}(t)}{\partial t} \tag{20}$$

where, being N_e the number of elements, the complementary length $L_{Ci}(t)$ is given by:

$$L_{Ci}(t) = L(t) - L_i(t) = L(t) \left[1 - \frac{i-1}{N_e} \right] \tag{21}$$

The flexural displacement can be represented by the following vector expression:

$$v = \mathbf{F}^T \mathbf{q}_e \tag{22}$$

where the shape functions and nodal variables are given by:

$$\mathbf{F} = \left\{ 1 - \frac{3\bar{x}^2}{l_e^2} + \frac{2\bar{x}^3}{l_e^3}, \bar{x} - \frac{2\bar{x}^2}{l_e} + \frac{\bar{x}^3}{l_e^2}, \frac{3\bar{x}^2}{l_e^2} - \frac{2\bar{x}^3}{l_e^3}, -\frac{\bar{x}^2}{l_e} + \frac{\bar{x}^3}{l_e^2} \right\}$$

$$\mathbf{q}_e = \left\{ v_1, \frac{\partial v_1}{\partial \bar{x}}, v_2, \frac{\partial v_2}{\partial \bar{x}} \right\}^T \tag{23}$$

It has to be mentioned that, l_e is time dependent, consequently the finite element expressions for the derivatives of variable v are:

$$\frac{\partial v}{\partial \bar{x}} = \frac{\partial \mathbf{F}^T}{\partial \bar{x}} \mathbf{q}_e$$

$$\frac{\partial^2 v}{\partial \bar{x}^2} = \frac{\partial^2 \mathbf{F}^T}{\partial \bar{x}^2} \mathbf{q}_e \tag{24}$$

$$\frac{\partial v}{\partial t} = \frac{\partial \mathbf{F}^T}{\partial t} \mathbf{q}_e + \mathbf{F}^T \frac{\partial \mathbf{q}_e}{\partial t}$$

Now, substituting (24) into expression (18), performing variational calculus, integrating in the time variables and arranging in terms of the vector of nodal variables, nodal velocities and nodal accelerations, one can arrive to the following element equation:

$$\mathbf{m}_e \frac{\partial^2 \mathbf{q}_e}{\partial t^2} + \mathbf{c}_{eq} \frac{\partial \mathbf{q}_e}{\partial t} + \mathbf{k}_{eq} \mathbf{q}_e = 0 \tag{25}$$

where $\mathbf{m}_e$, $\mathbf{c}_{eq}$ and $\mathbf{k}_{eq}$ are the elementary matrices of mass, equivalent damping and equivalent stiffness, respectively. The elementary mass matrix is given by:

$$\mathbf{m}_e = \int_0^{l_e(t)} J_{11}^\rho \mathbf{F}^T \mathbf{F} d\bar{x} \tag{26}$$

Whereas the elementary equivalent damping and equivalent stiffness matrices are given by:

$$\mathbf{c}_{eq} = \mathbf{c}_{e1} - \mathbf{c}_{e2} + \frac{\partial \mathbf{m}_e}{\partial t}$$

$$\mathbf{k}_{eq} = \mathbf{k}_{e0} - \mathbf{m}_{e1} - \mathbf{m}_{e2} + \frac{\partial \mathbf{c}_{e1}}{\partial t} \tag{27}$$

where

$$\mathbf{k}_{e0} = \int_0^{l_e(t)} J_{11}^{11} \frac{\partial^2 \mathbf{F}^T}{\partial \bar{x}^2} \frac{\partial^2 \mathbf{F}}{\partial \bar{x}^2} d\bar{x}$$

$$\mathbf{c}_{e1} = \int_0^{l_e(t)} J_{11}^\rho \left(\mathbf{F}^T \frac{\partial \mathbf{F}}{\partial t} + \frac{\partial L_{Ci}}{\partial t} \mathbf{F}^T \frac{\partial \mathbf{F}}{\partial \bar{x}} \right) d\bar{x}$$

$$\mathbf{c}_{e2} = \int_0^{l_e(t)} J_{11}^\rho \left(\frac{\partial \mathbf{F}^T}{\partial t} \mathbf{F} + \frac{\partial L_{Ci}}{\partial t} \frac{\partial \mathbf{F}^T}{\partial \bar{x}} \mathbf{F} \right) d\bar{x} \tag{28}$$

$$\mathbf{m}_{e1} = \int_0^{l_e(t)} J_{11}^\rho \left[\frac{\partial \mathbf{F}^T}{\partial t} \frac{\partial \mathbf{F}}{\partial t} + \frac{\partial L_{Ci}}{\partial t} \left(\frac{\partial \mathbf{F}^T}{\partial t} \frac{\partial \mathbf{F}}{\partial \bar{x}} + \frac{\partial \mathbf{F}^T}{\partial \bar{x}} \frac{\partial \mathbf{F}}{\partial t} \right) + \left(\frac{\partial L_{Ci}}{\partial t} \right)^2 \frac{\partial \mathbf{F}^T}{\partial \bar{x}} \frac{\partial \mathbf{F}}{\partial \bar{x}} \right] d\bar{x}$$

$$\mathbf{m}_{e2} = \int_0^{l_e(t)} J_{11}^\rho (L_{Ci} - \bar{x}) \frac{\partial V}{\partial t} \frac{\partial \mathbf{F}^T}{\partial \bar{x}} \frac{\partial \mathbf{F}}{\partial \bar{x}} d\bar{x}$$

It is clear that $\mathbf{k}_{e0}$ is the common structural stiffness matrix, but the other three matrices of $\mathbf{k}_{eq}$ are mass-dependent components of the equivalent stiffness of the sliding beam. The damping matrix is in general non-symmetric. If the motion is such that the mass enters to the system (i.e. extrusion), then matrix $\mathbf{c}_{eq}$ is positive definite, but if the mass is leaving the system (i.e. retraction), the matrix $\mathbf{c}_{eq}$ is negative definite.

After the assembling process, one can get the following expression:

$$\mathbf{M}\frac{\partial^2 \mathbf{Q}}{\partial t^2} + \mathbf{C}_{eq}\frac{\partial \mathbf{Q}}{\partial t} + \mathbf{K}_{eq}\mathbf{Q} = \mathbf{0} \tag{29}$$

where $\mathbf{M}$, $\mathbf{C}_{eq}$ and $\mathbf{K}_{eq}$ are the global matrices of mass, equivalent damping and equivalent stiffness, whereas $\mathbf{Q}$ is the global vector of nodal variables.

The damping matrix $\mathbf{C}_{eq}$ can be modified in order to account for structural damping as:

$$\mathbf{C}_{eq} = \mathbf{C}_1 - \mathbf{C}_2 + \frac{\partial \mathbf{M}}{\partial t} + \mathbf{C}_{RD} \tag{30}$$

The matrix $\mathbf{C}_{RD}$ corresponds to the system proportional Rayleigh damping given by:

$$\mathbf{C}_{RD} = \alpha\mathbf{M} + \beta\mathbf{K} \tag{31}$$

where $\mathbf{M}$ and $\mathbf{K}$ are the global mass and structural stiffness matrices, respectively; whereas parameters α and β are computed from two experimental modal damping functions (Bathe, 1982; Meirovith, 1997).

The Matlab solvers are employed to simulate numerically the finite element model, for this reason the equation (29) is represented in the following ODE form:

$$\mathbf{A}\frac{d\mathbf{W}}{dt} + \mathbf{B}\mathbf{W} = \mathbf{0} \tag{32}$$

where:

$$\mathbf{A} = \begin{bmatrix} \mathbf{C}_{eq} & \mathbf{M} \\ \mathbf{M} & \mathbf{0} \end{bmatrix}$$
$$\mathbf{B} = \begin{bmatrix} \mathbf{K}_{eq} & \mathbf{0} \\ \mathbf{0} & -\mathbf{M} \end{bmatrix} \tag{33}$$
$$\mathbf{W} = \left\{ \mathbf{Q}, \frac{d\mathbf{Q}}{dt} \right\}^T$$

3   NUMERICAL STUDIES

3.1   Convergence and Comparisons with other Approaches

In the following paragraphs convergence check and comparison between different approaches are performed. In these calculations the structural damping is neglected.

Figure 2 shows the tip displacements of four different discretization (with two, four, six and eight elements) of a isotropic beam tested by other authors (Al-Bedoor and Khulief, 1997),

whose properties are shown in Table 1. The deployment of the beam follows a profile for $L(t)$ given by:

$$L(t) = L_0 + V.t \tag{34}$$

where $L_0 = 1.8m$ is the initial length of the beam outside the hub, $V = 0.3m/s$ is the deployment velocity. For the simulation process, a tip displacement of -0.005 m and null velocities are imposed in the initial state vector.

Properties	Value
Total length L_T $[m]$	3.6
Flexural Stiffness J_{11}^{11} $[N/m^2]$	756.65
Mass per unit length J_{11}^{ρ} $[Kg/m]$	4.015

Table 1: Data for the aluminium beam tested

Figure 3 shows the time consumed in the calculation (in a Pentium IV computer with 3.2 GHz, 512 RAM) of the four models. As it can be seen from Figures 2 and 3, models with few element can reach acceptable results in reasonable short time.
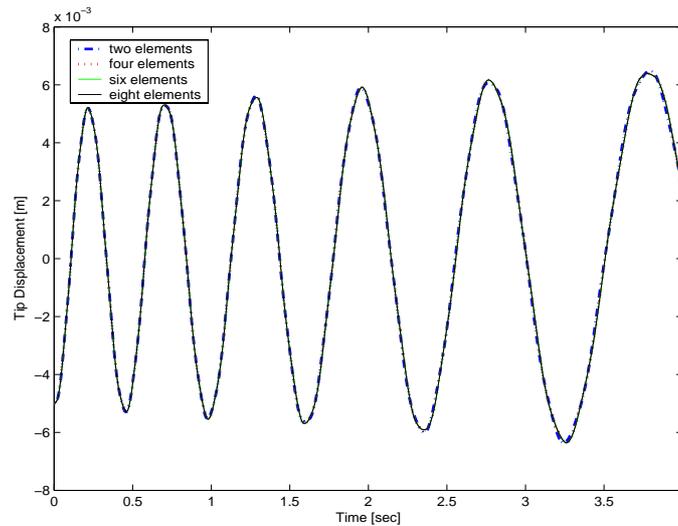

Figure 2: Response for different discretization cases.

Figure 4 shows the tip deflection of the previous isotropic beam, comparing the present formulation and the transition element formulation (Al-Bedoor and Khulief, 1997). Both approaches employed beam models with four finite element.

The tip deflections of the retracting beam are compared in Figure 5. Once again the present formulation and the transition element formulation (Al-Bedoor and Khulief, 1997) are compared. In this case the retracting pattern with the same form of expression (34), but with $L_0 = 3.0m$, $V = -0.3m/s$ and an initial tip displacement of $-10mm$. For this last calculation, a model with four elements was employed. An excellent agreement between the two approaches is observed.
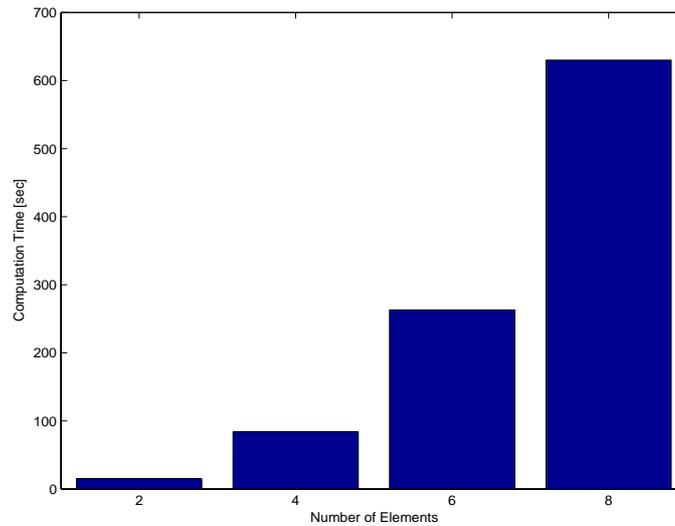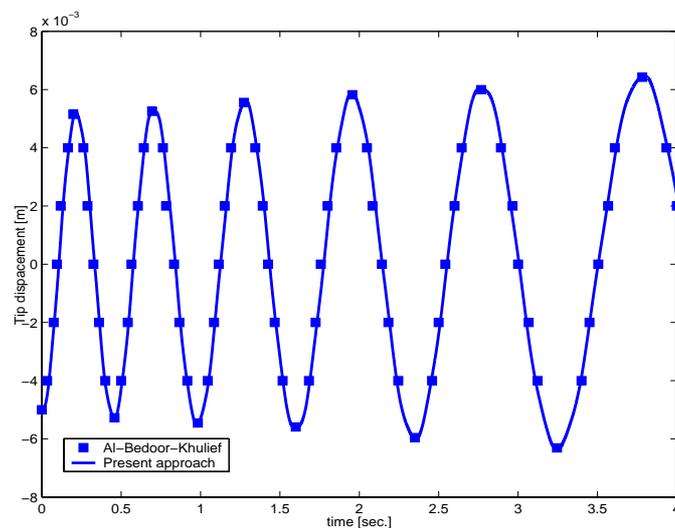
Figure 3: Computation time for different discretization cases.

Figure 4: Tip deflection of a deploying beam at $V = 0.3m/s$.

3.2 Simulation the Dynamics of Beams made of Functionally Graded Materials

In this paragraph an analysis of the dynamics of sliding beams with different configurations of Functionally Graded properties is performed. The beam for the studies performed in this paragraph is constructed by a material whose properties vary functionally from a stainless steel surface of SUS304 to a ceramic surface of Silicon Nitride. The basic properties of these components components (Reddy and Chin, 1998; Oh et al., 2003), are given in Table 2. For every simulation the beam has a total length $L_T = 3.6m$ and the cross-section has a mean radius $R_m = 0.025m$ m. and a wall thickness $e = 0.004m$.

As a first simulation, the two deployment profiles of expressions (35) and (36) are selected. In (35) L_0 is the initial free length of the beam, V is the sliding velocity and a is the acceleration. In (36) L_0 is the initial free length of the beam, τ and η are constants. The deployment pattern (35) produces the deployment of the beam with a constant acceleration and contains (34) as a particular case. The pattern (36) performs the deployment of the beam with time varying
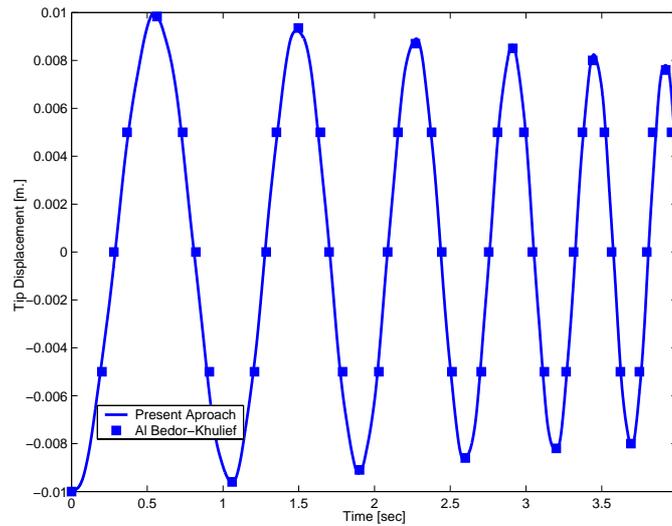
Figure 5: Tip deflection of a deploying beam at $V = -0.3m/s$

velocity and acceleration. Thus, under this pattern, the beam domain evolves with pulsatile velocity (between zero and η/τ) and sinusoidal acceleration.

$$L(t) = L_0 + V.t + \frac{at^2}{2} \tag{35}$$

$$L(t) = L_0 + \frac{\eta}{\tau} \left[t - \frac{\tau}{2\pi} Sin \left[\frac{2\pi}{\tau} t \right] \right] \tag{36}$$

Figures 6 and 7 show the tip displacement of a beam under the extrusion corresponding to deployment laws (35) and (36), respectively. For both simulations models with four elements and imposing an initial tip displacement of -5 mm. were employed and a functionally graded material with a ceramic outer surface and a metallic inner surface was adopted. No structural damping and temperature effects were considered. The properties for the deployment law (35) were $L_0 = 1m$, $V = 2m/s$ and $a = 3m/s^2$; whereas for deployment law (36), $L_0 = 1m$, $\eta = 0.7$ and $\tau = 0.2$. In both figures it is possible to see the high frequency oscillating deployment when the exponent $K = 0$, because the beam is totally made of ceramic which has high stiffness.

Properties	Material	p_0	p_{-1}	p_1	p_2	p_3
$E[N/m^2]$	SUS304	2.0104×10^{11}	0	3.0790×10^{-4}	-6.534×10^{-7}	0
	Si_3N_4	3.4843×10^{11}	0	-3.0700×10^{-4}	2.160×10^{-7}	-8.946×10^{-11}
ν	SUS304	0.3262	0	-2.0020×10^{-4}	3.797×10^{-7}	0
	Si_3N_4	0.2400	0	0	0	0
$\rho[kg/m^3]$	SUS304	8166	0	0	0	0
	Si_3N_4	2370	0	0	0	0

Table 2: Properties of Stainless Steel (SUS304) and Silicon Nitride (Si_3N_4)

It is easy to modify (Stylianou and Tabarrok, 1994) the finite element formulation in order to account for a lumped tip mass M_T. Just a lumped mass term has to be added in the tip node and the factor $J_{11}^\rho (L_{Ci} - \bar{x})$ in the matrix $\mathbf{m}_{e2}$ has to be changed by $(J_{11}^\rho (L_{Ci} - \bar{x}) + M_T)$.
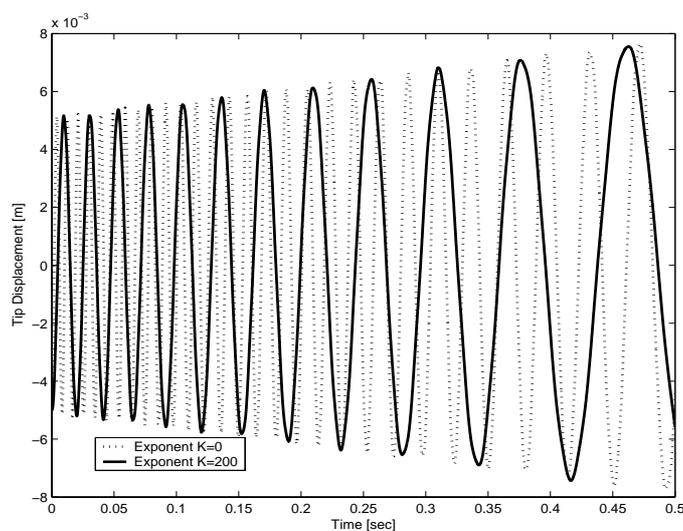
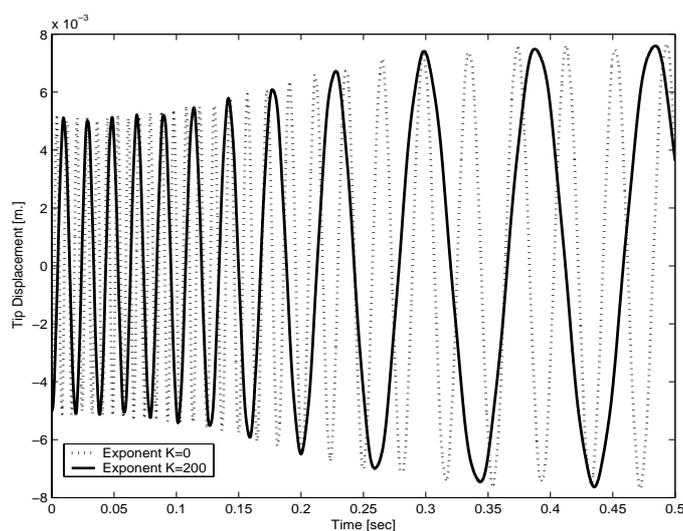Figure 6: Tip deflection of a deploying beam with a constant acceleration pattern.

Figure 7: Tip deflection of a deploying beam with a sinusoidal acceleration pattern

Figure 8 shows the time history of the tip displacement of a beam with an exponent of $K = 200$ deploying with the law (36), where $L_0 = 1m$, $\eta = 0.8$ and $\tau = 0.2$. In this study, the structural damping and the thermal effects are not considered . In one case a tip mass of $M_T = 1kg$ (which is approximately the 20% of the initial mass of the protruded bar, i.e. at t=0) is considered. As it was expected, the addition of a tip mass has the effect of lowering the frequency of oscillations during the extrusion.

A final analysis evaluates the effect of structural damping with the inclusion of tip mass. The coefficients α and β are calculated (Bathe, 1982) assuming for simulation purposes the damping coefficients ξ_1 and ξ_2 for the first and second frequencies respectively. Two cases are simulated, in the case 1, the damping coefficients are $\xi_1 = 1 \times 10^{-6}$ and $\xi_2 = 5 \times 10^{-6}$, in the case 2 the damping coefficients are $\xi_1 = 2 \times 10^{-5}$ and $\xi_2 = 1 \times 10^{-4}$. Figure 9 compares the time histories of the tip displacement for a beam with $K = 200$ and a tip mass of $M_T = 1kg$, taking into account and neglecting the structural damping. The deployment characteristics are
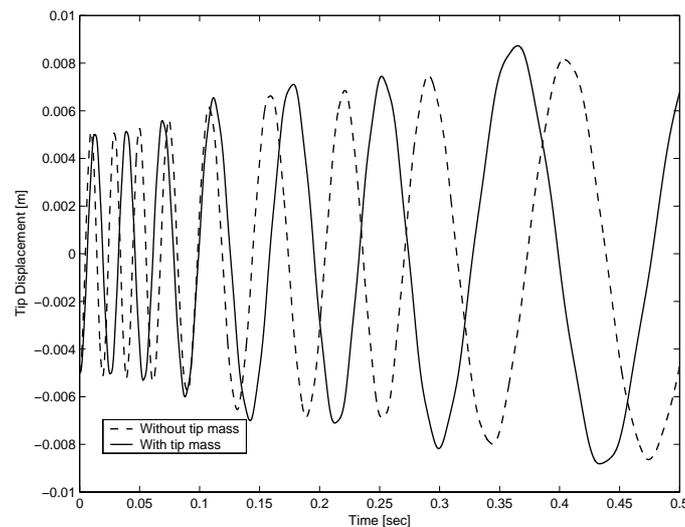
Figure 8: Effect of the tip mass on the Tip deflection for a sinusoidal acceleration pattern, $K = 200$

the same to those of the cases of Figure 8. As it can be seen, in the case 1 the motion is lightly damped, on the contrary the case 2 shows a more pronounced damping in the tip displacement of the system since the damping coefficients employed in the calculation of Rayleigh damping are twenty times greater than the ones employed in case 1.
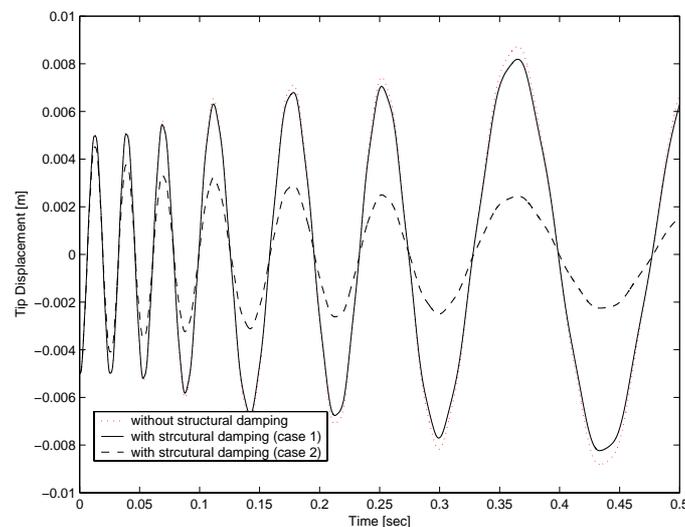

Figure 9: Tip deflection. Analysis of structural damping, $K = 200$

4 CONCLUSIONS

In this article a formulation for axially moving beams made of functionally graded materials was developed. The structural model is based on the Bernoulli-Euler hypotheses including the constitutive equations for a ceramic-metallic functionally graded material. The variation of properties along the wall thickness of the annular cross-section, follows a simple exponential law.

A finite element formulation was employed to simulate the dynamics of extruding and re-

tracting beams. This formulation considers the use of a beam element of variable length which showed a very good performance.

The finite element results obtained with this formulation for the tip displacement of a sliding beam, agrees well with the results published by other authors employing the assumed modes methods.

Two different patterns or deployment laws were tested in the protrusion of functionally graded beams. The variation of the properties by means of the exponent K was analyzed. The simulation results showed that the beam presents a high (low) oscillatory deployment when it is composed mainly by the ceramic (metallic) component.

As a final conclusion, this kind of model is quite useful for the analysis of deploying beam-like structures with specified deploying patterns, for both functionally graded and isotropic materials. Although the model presents a relative complexity in its formulation (due to the concept of element with variable length), it has a good computational performance.

5   ACKNOWLEDGEMENTS

REFERENCES

B.O. Al-Bedoor and Y.A. Khulief. Vibrational motion of an elastic beam with prismatic and revolute joints. *Journal of Sound and Vibration*, 190(2):195–206, 1996.

B.O. Al-Bedoor and Y.A. Khulief. General planar dynamics of a sliding flexible link. *Journal of Sound and Vibration*, 207(5):641–661, 1997.

K.J. Bathe. *Finite Element procedures in Engineerign Analysis*. Prentice-Hall, Englewood Cliffs, New Jersey, 1982.

K. Behdinan, M. Stylianou, and B. Tabarrok. Dynamics of flexible sliding beams - non-linear analysis part i: Formulation. *Journal of Sound and Vibration*, 208(4):517–539, 1997a.

K. Behdinan, M. Stylianou, and B. Tabarrok. Dynamics of flexible sliding beams - non-linear analysis part ii: Transient response. *Journal of Sound and Vibration*, 208(4):541–565, 1997b.

V.H. Cortinez and M.T. Piovan. Vibration and buckling of composite thin walled beams with shear deformability. *Journal of Sound and Vibration*, 258(4):701–723, 2002.

E. Imanishi and N. Sugano. Vibration control of cantilever beams moving along the axial direction. *JSME International Journal Series C*, 46(2):527–532, 2003.

R. Kadoli and N. Ganesan. Buckling and free vibration analysis of functionally graded cylindrical shells subjected to a temperature-specified boundary condition. *Journal of Sound and Vibration*, 289:450–480, 2006.

B.D. McIver. Hamilton's principle for a system of changing mass. *Journal of Engineering Mathematics*, 7:249–261, 1973.

L. Meirovith. *Principles and Techniques of Vibrations*. Prentice Hall, Upper Saddle River, New Jersey, 1997.

S.Y. Oh, L. Librescu, and O. Song. Thermoelastic modeling and vibrations of functionally graded thin walled rotating blades. *AIAA Journal*, 41(10):2051–2060, 2003.

G.N. Praveen, C.D. Chin, and J.N. Reddy. Thermoelastic analysis of functionally graded ceramic-metal cylinder. *Journal of Engineering Mechanics*, 125:1259–1267, 1999.

J.N. Reddy and C.D. Chin. Thermomecanical analysis of functionally graded cilinders and plates. *Journal of Thermal Stresses*, 21:593–626, 1998.

M. Stylianou and B. Tabarrok. Finite element analysis of an axially moving beam, part i: Time integration. part ii: Stability analysis. *Journal of Sound and Vibration*, 178(4):433–473, 1994.

Y. Tanigawa. Some basic thermoelastic problems for nonhomogeneous structural materials. *Applied Mechanics Review*, 48:287–300, 1995.

R.J. Theodore, J.H. Arakeri, and A. Ghosal. The modelling of axially translating flexible beams. *Journal of Sound and Vibration*, 191(3):363–376, 1996.